# Faraday Discussions

Accepted Manuscript

**Faraday Discussions**

**Royal Society of Chemistry**

ROYAL SOCIETY
OF CHEMISTRY

www.rsc.org/faraday_d

# 3 Raising the Barrier for Photoinduced DNA Charge Injection with a Cyclohexyl Artificial Base Pair[†]

**Arunoday P. N. Singh, Michelle A. Harris, Ryan M. Young, Stephen**
<sub>5</sub> **A. Miller, Michael R. Wasielewski, and Frederick D. Lewis[a,b]**

The effects of an artificial cyclohexyl base pair on the quantum yields of fluorescence and dynamics of charge separation and charge recombination have been investigated for several synthetic DNA hairpins. The hairpins
<sub>10</sub> possess stilbenedicarboxamide, perylenediimide, or naphthalenediimide linkers and base-paired stems. In the absence of the artificial base pair hole injection into both adenine and guanine purine bases is exergonic and irreversible, except in the case of stilbene with adenine for which it is slightly endergonic and reversible. Insertion of the artificial base pair
<sub>15</sub> renders hole injection endergonic or isoergonic except in the case of the powerful naphthalene acceptor for which it remains exergonic. Both hole injection and charge recombination are slower for the naphthalene acceptor in the presence of the artificial base pair than in its absence. The effect of an artificial base pair on charge separation and charge recombination in
<sub>20</sub> hairpins possessing stilbene and naphthalene acceptor linkers and a stilbenediether donor capping group has also been investigated. In the case of the stilbene acceptor-stilbene donor capped hairpins photoinduced charge separation across six base pairs is efficient in the absence of the artificial base pair but does not occur in its presence. In the case of the
<sub>25</sub> naphthalene acceptor-stilbene donor capped hairpins the artificial base pair slows but does not stop charge separation and charge recombination, leading to the formation of long-lived charge separated states.

## 1 Introduction

The dynamics of photoinduced charge separation in electron donor–acceptor
<sub>30</sub> systems is dependent upon the change in free energy, the distance between the donor and acceptor, the solvent polarity, and the presence or absence of an intervening spacer or bridge.[1-4] Investigations of the dynamics of photoinduced charge injection in DNA have employed chromophores which are stacked with the base pairs of DNA by means of intercalation, located with a duplex by replacement of a natural base
<sub>35</sub> with a base surrogate, or covalently attached to the end of a duplex as a hairpin linker or capping group.[5-7] Genereux and Barton[8] have suggested that the yields and rates of charge injection and migration reflect "…the relative stacking of the donor and acceptor with the DNA duplex." Relatively few studies in which the donor or acceptor chromophore and base were purposely separated have been reported. We
<sub>40</sub> previously investigated the effects of interposing one or more G-G base pairs between a stilbenediether hairpin linker (SD electron donor, Chart 1a) and an A-T base pair (thymine electron acceptor) on the SD singlet lifetime. An increase in
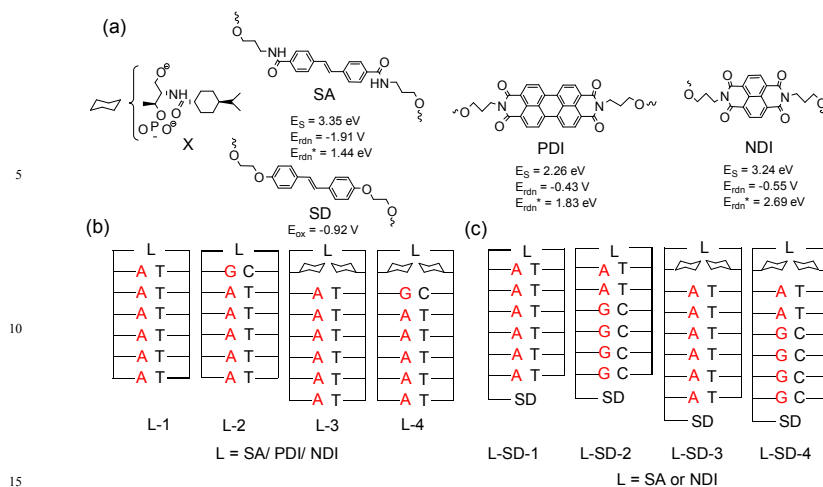
**Chart 1**: (a) Structures of the artificial cyclohexane base X, structures, singlet energies and reduction potentials of stilbenedicarboxamide (SA), perylenediimide (PDI), and naphthalenediimide (NDI) hairpin linkers, and the structure and oxidation potential of the stilbenediether (SD) hairpin capping group; (b) structures of simple hairpins with and without cyclohexane base pairs (X-X); (c) structures of SD-capped hairpins having SA or NDI linkers.

[1]SD* lifetime was observed for 1 or 2 intervening G-G base pairs, in accord with the inability of G to serve as an electron acceptor.[9] Kawai et al. have reported that reversing the initial A-T base pair in a poly(A)-poly(T) sequence increases the lifetime and quantum yield of the charge separated states formed upon hole injection from singlet naphthalene imide.[10] However, the dynamics of charge injection in these systems has not been investigated.

Recently Kashida et al. have reported that insertion of an artificial base pair composed of cyclohexyl base surrogates (X-X, Chart 1a) on either side of the perylenediimide (PDI) chromophore in the interior of a synthetic duplex results in reduction of fluorescence quenching by the adjacent G-C base pairs.[11, 12] The insulating artificial base pairs serve both to stabilize the modified duplex and to enhance the fluorescence of the PDI chromophore. A single X-X partially restores the PDI fluorescence; however, a cluster of three insulating base pairs on both sides of PDI restores essentially all of its fluorescence. A similar decrease in fluorescence quenching was observed upon insertion of X-X base pairs between the tetramethylrhodamine chromophore and neighboring G-C base pairs.[13]

We report here the results of an investigation of the effects of an artificial X-X base pair on the efficiency and dynamics of hole injection and charge recombination from a linker chromophore to a neighboring base pair in several DNA hairpins (Chart 1b). The driving force for hole injection can be varied both by changing the base pair from A-T to G-C and by changing the hairpin linker from stilbenedicarboxamide (SA) to perylenediimide (PDI) or naphthalenediimide (NDI, Chart 1a). In addition, hole transport from a SA or NDI linker to a stilbenediether (SD) capping group located at the opposite end of capped hairpins (Chart 1c) has been investigated. Hole transport across an X-X base pair requires that this process be exergonic by ca. 0.4 eV. This energy requirement is similar to that for bimolecular electron transfer in a solvent-separated donor-acceptor system.

## 2 Experimental

DNA conjugates were prepared and purified as previously described.[14, 15] The stilbenedicarboxamide,[16] naphthalenediimide,[17] and perylenediimide[18] linkers were prepared by literature methods. The cyclohexane base surrogate was prepared by the method of Kashida et. al.[11, 12] Conjugates were characterized by their UV, fluorescence, circular dichroism (CD), and mass spectra. Values of m/z obtained from MALDI-TOF mass spectrometry and thermal dissociation temperatures ($T_m$) for the hairpins and capped hairpins are reported in Electronic Supporting Information (ESI, Table 1). UV, fluorescence, CD, thermal dissociation and transient absorption experiments were performed in phosphate buffer (10 mM phosphate, 0.1 M NaCl, pH 7.2) for SA and NDI samples and in water (pH 7.2) for PDI samples. Fluorescence spectra were recorded for SA and NDI samples (optical density of 0.05 at 350 nm) in 1 mL buffer by exciting at 350 nm and for PDI samples (optical density of 0.05 at 495 nm) in 1 mL of water by exciting at 496 nm. Fluorescence quantum yields ($\Phi_f$) were determined relative to the quantum yield of quinine sulfate or fluorescein.[19] CD spectra of the hairpins and capped hairpins conjugates were recorded on Jasco J-815 CD spectrometer and are shown in Figure S1 (ESI).

Femtosecond transient absorption spectra were obtained using setups previously described.[20, 21] The samples were prepared in 2 mm cuvettes and excited with 1 μJ per pulse at 350, 400, and 545 nm for SA-, NDI-, and PDI-hairpins, respectively. Nanosecond transient absorption (nsTA) spectra were obtained using a femtosecond excitation beam (TOPAS-White, Light-Conversion, Ltd.) tuned to 350 nm pumped by an amplified femtosecond laser previously described[21] at 1 μJ per pulse and probed by a commercial spectrometer (EOS, Ultrafast Systems) utilizing a photonic crystal fiber ultra-broadband probe source. The experimental time resolution is approximately 600 ps with a time window out to 220 μs. The pump polarization in the nsTA experiment was randomized to remove rotational dynamics. Longer kinetics were obtained using a separate nsTA setup exciting the sample in a 1 cm cuvette with 7 ns, 1.6 mJ, 355 nm pulses using the attenuated frequency-tripled output of a Continuum Precision II 8000 Nd:YAG laser operating at 10 Hz. The probe pulse, generated using a xenon flashlamp (EG&G Electro-Optics FX-200), and pump pulse are overlapped on the sample with the pump being focused to a spot size slightly larger than the probe. Kinetic traces were observed at 485 nm and 535 nm using a 416 nm long-pass filter, a monochromator, and photomultiplier tube (Hamamatsu R928) with high voltage applied to only 4 dynodes. Kinetic traces are recorded with a LeCroy Wavesurfer 42Xs oscilloscope interfaced to a customized LabVIEW program (LabVIEW v. 8.6.1). Each kinetic trace is representative of an average of 100 shots over a varying time window of 0.1 to 5 ms depending on the decay time constant of the process. For both nsTA experiments, solutions were deoxygenated by bubbling with nitrogen for 30 minutes. All transient absorption samples were stirred during the experiment to minimize degradation. The data was analyzed using a multiexponential single wavelength fit with an instrument response function as well as using single value decomposition global analysis as previously described.[22]
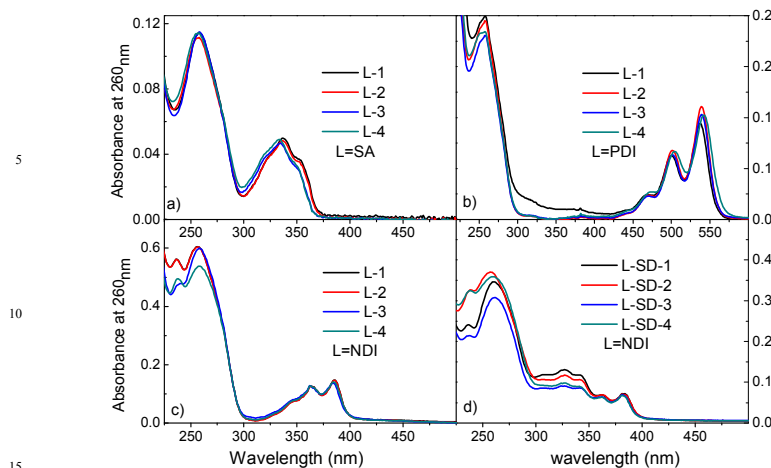
**Fig. 1** UV/visible absorption spectra (normalized) of hairpins **L-1-4** and capped hairpins **NDI-SD-1-4** in phosphate buffer (10 mM phosphate, pH 7.2, with 0.1 M NaCl except for **PDI-1-4**).

## 3 Results and discussion

### A. Steady state spectra of DNA hairpin conjugates

DNA hairpins **L-1** and **L-2** possessing SA, PDI, and NDI linkers were prepared by methods that we have previously described (see Experimental). The hairpins **L-3** and **L-4** were prepared by inserting the insulating cyclohexane base pair X-X between the linker chromophores and the adjacent chromophore using the method of Kahida and co-workers for the preparation and incorporation of the *trans*-4-isopropylcyclohexyl derivative of D-throninol.[11, 12] The CD spectra of the hairpins are shown in Figure S1 (ESI). The short-wavelength maxima and minima (200-300 nm) are consistent with B-DNA base-paired structures.[23] Minima at longer wavelengths are attributed to induced CD of the linker chromophores.[24]

The UV-vis absorption spectra of the hairpins **L-1** and **L-2** in phosphate buffer all consist of a long-wavelength band characteristic of the linker chromophore and a more intense band with a maximum around 260 nm attributed to overlapping absorption of the nucleobases and the linker chromophore (Figure 1). The long-wavelength bands of hairpins **L-3** and **L-4** are blue-shifted with respect to those for **L-1** and **L-2**. The extent of the blue shift is larger for the SA linker (ca. 5 nm) than for either PDI or NDI (2 ± 1 nm). The long-wavelength band the PDI-linked hairpins have a strong vibronic progression characteristic of the PDI monomer, as previously observed for PDI-linked hairpins in the absence of added NaCl.[25] Added 100 mM NaCl effects PDI hairpin dimerization resulting in a change in the long-wavelength absorption band from that of PDI monomer to PDI dimer.[25] No changes in the absorption spectra of the SA or NDI hairpins are observed upon addition of 100 mM NaCl, consistent with the absence of salt-induced dimerization for these smaller, less hydrophobic chromophores.

The fluorescence spectra of the linked hairpins are shown in Figure 2 and their fluorescence quantum yields are reported in Table 1. The fluorescence quantum yields of all of the **L-2** hairpins are low (≤ 0.002) indicative of efficient fluorescence quenching of all three chromophores by neighboring guanine. The fluorescence
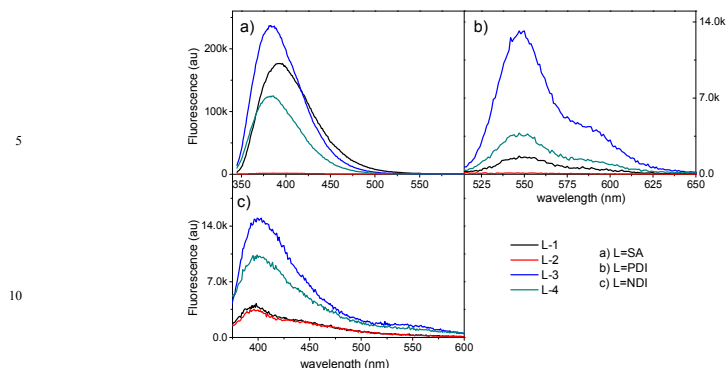
**Fig. 2** Fluorescence spectra of hairpins **L-1-4** in phosphate buffer (10mM phosphate, pH 7.2, with 0.1 M NaCl except for **PDI-1-4**).

**Table 1:** Fluorescence quantum yields ($\Phi_{fl}$), calculated free energies for charge separation ($\Delta G_{cs}$), and transient decay times obtained from global analysis assigned to singlet decay ($\tau_s$), and charge recombination ($\tau_{cr}$) (see Chart 1 for hairpin structures).[a] Values in *()* are the relative population of each component based on area of the singlet excited and anion absorption features of the relative acceptor.

| Hairpin | $\Phi_{fl, \%}$[b] | $\Delta G_{cs}$, eV[c] | $\tau_s$, ps[d] | $\tau_{cr}$, ps[e] |
|---|---|---|---|---|
| SA–1 | 23.0 | +0.10 | 3.8 *(32)*, 49 *(22)*, 2300 *(46)*[e] | |
| SA–2 | 0.20 | −0.15 | 0.8 *(55)* | 23*(45)* |
| SA–3 | 18.5 | | 62 *(76)*, 1000 *(24)*[f] | |
| SA–4 | 0.60 | | 2.9 *(30)*, 46 *(41)* | 480 *(29)* |
| PDI–1 | 0.33 | −0.05 | 13(78), 52 (16) | 900 *(6)* |
| PDI–2 | 0.03 | −0.30 | *1.2 (88)* | 18 *(10)*, 800 *(2)* |
| PDI–3 | 2.6 | | *0.9 (79), 34 (11), 1000 (10)* | |
| PDI–4 | 0.77 | | 2.4 *(62)*, 42 *(14)*, 1300 *(24)* | |
| NDI–1 | 0.14 | −1.10 | <0.2 | 7.1 *(91)*, 73 *(7)*, 2700 *(2)* |
| NDI–2 | 0.12 | −1.40 | <0.2 | 0.5 *(83)*, 16 *(17)* |
| NDI–3 | 0.51 | | <0.5, 5.5 *(81)* | 67 *(9)*, >5000 *(10)* |
| NDI–4 | 0.37 | | 1.2 *(70)*, 19 *(30)* | |

a Measurements for SA and NDI in aqueous buffer (0.1 M NaCl and 10 mM sodium phosphate, pH 7.2) and for PDI without added NaCl. b Quinine sulfate and fluorescein were used as standards. λex 350 nm for SA and NDI samples and λex 496 nm for PDI. c Free energy for charge separation calculated using eq. 1 with data in Chart 1a. d Transient decay times assigned to singlet state decay. e Transient decay times assigned to charge recombination. f Singlet decay attributed to delayed fluorescence.

quantum yields for **PDI-1** and **NDI-1** are also low. The large fluorescence quantum yield and long fluorescence lifetime for **SA-1** is attributed to delayed fluorescence from the reversibly formed $SA^{-\cdot}$-$A^{+\cdot}$ radical ion pair.[26, 27] The free energy for formation of the radical ion pair from the locally excited linker singlet state can be calculated using Weller's equation;[28]

$$\Delta G_{et} = E_{ox} - E_{rdn} - E_s + \delta \qquad (1)$$

where $E_S$ and $E_{rdn}$ are the singlet energy and reduction potential of the chromophore (Chart 1 a)[29] $E_{ox}$ is the oxidation potential of the adjacent purine base, and $\delta$ is a solvent-dependent term which corrects for the difference in energy between the contact radical ion pair and free radical ions.[30] Assuming a highly polar
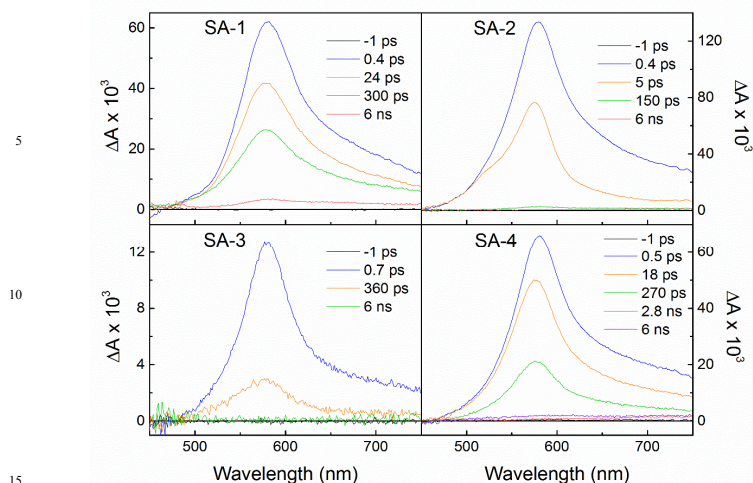
**Fig. 3** Transient absorption spectra for SA-linked hairpins **SA–1–4** in phosphate buffer (10 mM phosphate, 0.1 M NaCl, pH 7.2). Selected spectra at −1 ps, a time point immediately after the instrument response, points at $\tau*6$, and a final time point as the extent of the time collected.

environment for the linker and adjacent base pair, a value of $\delta = + 0.05$ can be assumed. We have previously employed the values of $E_{ox}$ for oxidation of the nucleotides reported by Seidel et al. for polar aprotic solvents (1.24 V and 1.69 V vs. SCE for G and A, respectively).[31] However, these values appear to overestimate the difference in the values for G and A within a base paired duplex.[32, 33] Thus we have adopted a lower value for A ($E_{ox} = 1.44$ V) in calculating the values of $\Delta G_{cs}$ reported in Table 1. In the case of **PDI-1** and **PDI-2** the values of $\Delta G_{cs}$ have been adjusted to be consistent with a prior report that hole injection from $^1$PDI* to A-T is approximately isoergic.[34] State energy diagrams showing the energies of the singlet excited states and radical ion pairs relative to the ground state energy for the three linkers are shown in Scheme 1a-c.

As is the case for the absorption spectra, the maxima of the fluorescence spectra of hairpins **L-3** and **L-4** are blue shifted with respect to those for **L-1** and **L-2**, the largest shifts (ca. 7 nm) being observed for the SA-linked hairpins **SA-3** and **SA-4** (Figure 2). The fluorescence spectra of **PDI-3** and **PDI-4** and **NDI-3** and **NDI-4** display long-wavelength shoulders, consistent with emission from a locally excited singlet state of the linker, as previously observed by Kashida and co-workers for duplex possessing a PDI base pair surrogate with X-X base pairs on both sides.[11, 12] We assume that the blue-shifted structureless emission from **SA-3** and **SA-4** also can be attributed to the locally-excited SA linker. Large increases in $\Phi_f$ are observed for **SA-4** vs. **SA-2** and for **PDI-4** vs. **PDI-2**, but not for **NDI-4** vs. **NDI-2**. Thus the X-X base pair attenuates fluorescence quenching by G to a much greater extent for SA and PDI chromophores than for the more powerful electron acceptor NDI. The same is true for quenching by A, for which the X-X base pair has the smallest effect on the extent of quenching of NDI in **NDI-3** vs. **NDI-1**. The average of the two transient decay times for **SA-3** (*vide* infra, Table 1) is similar to the fluorescence decay time for the diol derivative of the SA linker in methanol (350 ps) and thus is assigned to fluorescence of unquenched $^1$SA*.[26]
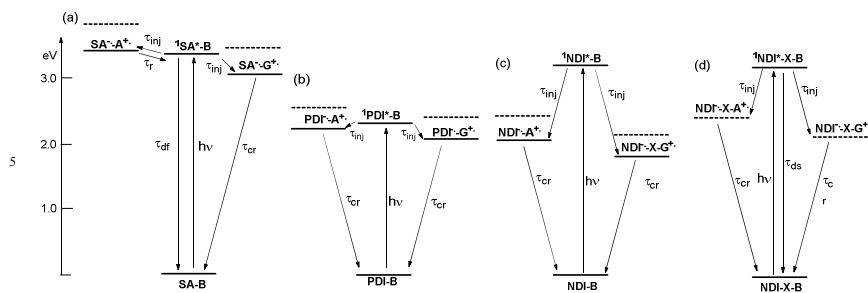
**Scheme 1.** Energetics and dynamics for hole injection and charge recombination in simple hairpins possessing (a) SA, (b) PDI, or (c) NDI linkers (B = purine base A or G). Dashed lines indicate the higher energy of the radical ion pair when separated by an X-X artificial base pair. (d) Energetics and dynamics for NDI hairpins possessing an artificial X-X base pair.

**B. Dynamics of hole injection and charge recombination in simple hairpins**

**1. Stilbenedicarboxamide-linked hairpins**

The transient absorption spectra of hairpins **SA-1-4** are shown in Figure 3. Femtosecond transient absorption spectroscopy have previously been reported for the SA-linked hairpin **SA-1** and for a hairpin similar to **SA-2** in which the G-C bases are exchanged (G is located in the poly(A) arm).[14] Global analysis of the transient decays for **SA-1** and **SA-2** provides the values of $\tau_s$ and $\tau_{cr}$ and the population fractions for each decay component are reported in Table 1. In the case of **SA-1**, the absence of a well-resolved 525 nm shoulder is attributed to an unfavorable equilibrium for conversion $^1SA^*$ to $SA^-$ (Scheme 1a). The triexponential decay of the transient absorption has decay times similar to those for the fluorescence of **SA-1** and is attributed to delayed fluorescence of $^1SA^*$.[26] The fast component of 575 nm decay for **SA-2** is accompanied by the growth of a 525 nm shoulder attributed to the formation of $SA^-$ and the slow component is attributed to charge recombination (Scheme 1a). The values of $\tau_s$ and $\tau_{cr}$ for **SA-2** are the same as those reported in our initial investigation of a hairpin having an adjacent G-C base pair.[14]

In the case of **SA-3** the absence of a fast component of transient decay and growth of a 525 nm shoulder indicate that hole injection does not occur. The two transient decays are assigned to $^1SA^*$ and plausibly reflect the existence of two or more ground state conformaitons (Table 1). Their weighted average decay time is ca. 300 ps, similar to that for the singlet excited state of the dihydroxypropyl derivative of the SA linker.[14] In the case of **SA-4**, insertion of an X-X base pair between SA and the G-C base pair results triexponential decay of the transient spectrum. The shortest-lived component assigned to decay of $^1SA^*$ has a value of $\tau_s$ that is ca. 4 times longer than that for **SA-2**, consistent with slower hole injection for **SA-4**. The second shortest component is also tentatively assigned to $^1SA^*$. The longest-lived decay component is assigned to charge recombination based on the appearance of a 525 nm shoulder at long delay times. Its decay time is ca. 20 times longer than that for **SA-2**. Thus the presence of the X-X base pair results in a decrease in the rate constants for both hole injection and charge recombination.

The presence of the X-X base pair is expected to have an effect on the energetics of hole injection similar to the presence of a non-polar solvent molecule located between the donor and acceptor on photoinduced charge separation. The barrier for electron tunneling through fluid solvents is known to be solvent-dependent.[35, 36] Farid et al. estimate that for highly exergonic charge separation in polar solvents
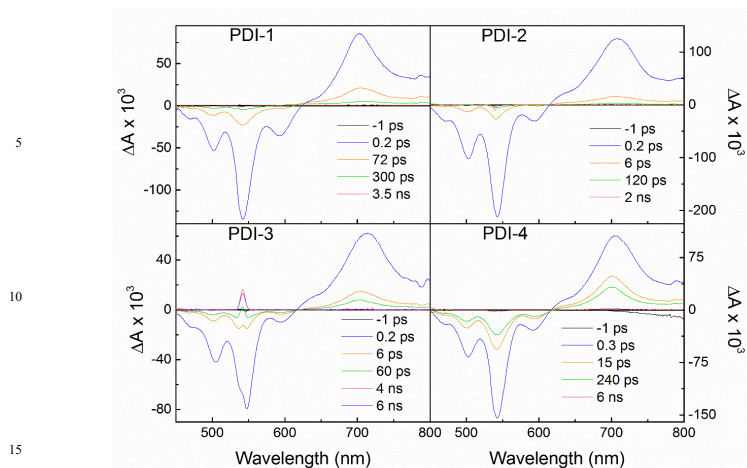
**Fig. 4** Femtosecond transient absorption spectra for PDI-linked hairpins **PDI−1−4** in water. Selected spectra at −1 ps, a time point immediately after the instrument response, points at τ*6, and a final time point as the extent of the time collected.

$(ΔG_{et}$ more negative than 0.4 eV), electron transfer can proceed directly to the solvent separated radical ion pair bypassing the contact radical ion pair.[30] Assuming a tunneling barrier of ca. 0.4 eV for the X-X base pair, electron injection for **SA-3** would become highly endergonic and thus unlikely to occur and electron injection for **SA-4** would become slightly endergonic and hence reversible (Scheme 1a, dashed lines), in accord with our experimental results. Grozema et al. estimate a larger value of ca. 0.6 eV for the difference in energy between a $SA^{-.}A^{+.}$ contact radical ion pair and a $SA^{-.}AA^{+.}$ radical ion pair in which the charges are separated by a single A-T base pair.[37] Delocalization of the positive charge within an A-track and increased solvent stabilization of the separated vs. contact radical ion pair may reduce this value.

**2. Perylenediimide-linked hairpins**

The transient spectra of hairpins **PDI-1** and **PDI-2** have previously been investigated in aqueous buffer containing 100 mM NaCl.[38] In the presence of added NaCl these hairpins the equilibrium between hairpin monomer and dimer favors the dimer and thus the results of our prior investigation pertain to the behavior of the head-to head PDI-PDI hairpin dimers.[25] We have repeated these measurements in the absence of added NaCl, under which conditions the hairpins exist predominantly as the base-paired monomer, as evidenced by their UV, fluorescence, and CD spectra (Figures 1b, 2b and S1b).

The transient absorption spectra of hairpins **PDI-1-4** are shown in Figure 4. At short delay times the spectra resemble those of DNA hairpins containing a PDI base surrogate with neighboring base pairs on both sides, having positive absorption bands with maxima near 690 nm and negative bands near 485, 530, and 580 nm (Figures 4).[34] The positive band is assigned to absorption of $^1$PDI*. The negative bands near 485 nm and 580 nm are assigned to the ground state depopulation of PDI and $^1$PDI* stimulated emission, respectively, while the negative band near 530 nm is assigned to overlapping ground state depopulation and stimulated emission.[39] In the case of the PDI base surrogate having adjacent A-T or G-C base pairs, the
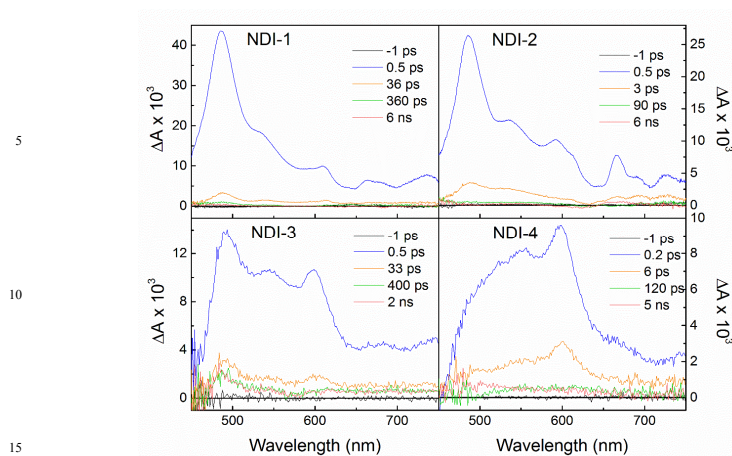
**Fig. 5** Femtosecond transient absorption spectra for NDI-linked hairpins **NDI–1–4** in phosphate buffer (10 mM phosphate, 0.1 M NaCl, pH 7.2). Selected spectra at −1 ps, a time point immediately after the instrument response, points at τ*6, and a final time point as the extent of the time collected.

absorption band undergoes a time-dependent red shift assigned to the formation of PDI[.−]. Little or no change in band shape is observed for **PDI-1-4** and thus we assume that either no change in the absorption band shape occurs upon hole injection or that hole injection is inefficient.

Global analysis of the transient decays of **PDI–1** provides decay times assigned to the reversibly formed singlet state, in accord with the behavior of a hairpin with a PDI base surrogate and neighboring A-T base pairs.[40] The minor long lived decay component is assigned to the small amount of PDI[.−]–A[+.] contact radical ion pair that undergoes charge separation prior to charge recombination. In the case of **PDI–2** exergonic charge separation is more rapid than for **PDI–1** and charge recombination occurs mainly via the short lived contact radical ion pair. In the case of **PDI–3** and **PDI–4** there is no evidence of the occurrence of hole injection to form a long lived radical ion pair separated by a X–X base pair. The observation of multiple exponential single state decay suggests that [1]PDI* may exist in multiple ground state conformations, as is the case for [1]SA* in hairpins **SA–3** and **SA–4.**

### 3. Naphthalenediimide-linked hairpins

We previously reported the dynamics of hole injection and charge recombination for hairpins having A-T and G-C base pairs adjacent to the NDI linker with the purine located in the poly(T) hairpin arm.[41] Majima et al. have investigated photoinduced charge separation in NDI-linked hairpins separated by 4-8 A-T base pairs from a phenothiazine (PTZ) hole acceptor by means of nanosecond laser spectroscopy.[42] They observed no long-lived NDI[.−] transients (>100 ns) in the absence of the PTZ hole acceptor. Curiously, whereas there have several nanosecond transient absorption studies of NDI-DNA conjugates, the femtosecond transient spectroscopy of these systems has not been well characterized.

The time resolved transient absorption spectra of the NDI diol in deoxygenataed methanol solution obtained with a 330 nm exiting pulse are shown in Figure S2 (ESI). A single band with a maximum at 590 nm assigned to [1]NDI* is formed during the pump pulse and decays with a time constant of 14 ± 5 ps to a much weaker band with a maximum near 480 nm and a tail extending to longer

wavelengths. The later band does not decay on the time scale of our measurements and is assigned to $^3$NDI*. The transient absorption spectra of singlet and triplet NDI and the singlet decay time are similar to those reported for an *N,N*-dialkyl NDI derivative in chloroform solution.[43]

5    The transient absorption spectra of **NDI-1-4** are shown in Figure 5 and the decay times obtained from global analysis are reported in Table 1. In the case of **NDI-1-2** the highly structured spectra assigned to NDI$^-$ are formed during the laser pump pulse, indicative of ultrafast electron transfer from the adjacent base pair.[44] The bandshapes of these spectra remain unchanged during the lifetime of NDI$^-$. Fast
10  decay of $^1$NDI* is consistent with the low fluorescence quantum yields for **NDI-1** and **NDI-2** (Table 1). The multi-exponential decays of the NDI$^-$ spectra are assigned to charge recombination. The charge recombination times obtained from global fitting of the **NDI-1**$^-$ and **NDI-2**$^-$ transient spectra are reported in Table 1. The faster decays for **NDI-2**$^-$ vs. **NDI-1**$^-$ are attributed to the smaller energy gap for
15  charge recombination of **NDI-2**$^-$ (Scheme 1c). The small component of long-lived decay for **NDI-1**$^-$ is assigned to charge recombination from separated radical ion pairs, formed upon transport of the hole beyond the first A-T base pair. The absence of a long-lived decay component for **NDI-2**$^-$ is consistent with hole localization on guanine.

20  The presence of an X-X artificial base pair between NDI and the adjacent natural base pair results in a pronounced change in the appearance of the transient absorption spectra of **NDI-3** and **NDI-4**. At short times, the absorption band at 595 nm assigned to $^1$NDI* (Figure S2, ESI) is a prominent feature of the transient spectra. The short-lived decay component of the $^1$NDI* transient spectra is assigned
25  to a combination of singlet nonradiative decay and hole injection (Scheme 1d) and is faster for **NDI-4** than for **NDI-3**. The NDI$^-$ decay times for **NDI-3** and **NDI-4** assigned to charge recombination are similar to those for hairpins **NDI-1** and **NDI-2**, respectively, but are lacking the dominant short-lived components observed for **NDI-1** and **NDI-2**. Plausibly, such short-lived decay components are competitive
30  with charge separation, resulting in inverted kinetics, thus accounting for the weak NDI$^-$ transient absorption spectra observed for **NDI-3** and **NDI-4**. The likelihood of competition between singlet decay and hole injection for $^1$NDI* and of inverted kinetics for charge recombination of NDI$^-$ makes it difficult to accurately determine the effect of the X-X base pair on the dynamics of hole injection and charge
35  recombination.

**C. Dynamics of hole injection, hole transport, and charge recombination in stilbenediether capped hairpins**

**1. Stilbenedicarboxamide-linked capped hairpins**
The efficiency and dynamics of charge separation for the SA-capped hairpins **SA-**
40  **SD-1** and **SA-SD-2** (Chart 1c) have previously been investigated by means of femtosecond time-resolved transient absorption spectroscopy.[45] Values of $\Phi_{cs}$ for these capped hairpins are reported in Table 2. The higher quantum yield for the diblock purine sequence in **SA-SD-2** was attributed to decreased charge return and charge recombination in the SA$^-$/A$^+$ contact radical ion pair as a consequence of the
45  lower oxidation potential of G vs. A (Scheme 2b vs. 2a). Charge separation times $\tau_{cs}$ for formation of the SA$^-$A$_6$SD$^+$ and SA$^-$A$_2$G$_4$SD$^+$ charge-separated states and the charge recombination time $\tau_{cr}$ for SA$^-$A$_6$SD$^+$ are reported in Table 2. The slow charge recombination for SA$^-$A$_6$SD$^+$ is attributed to a single step tunneling
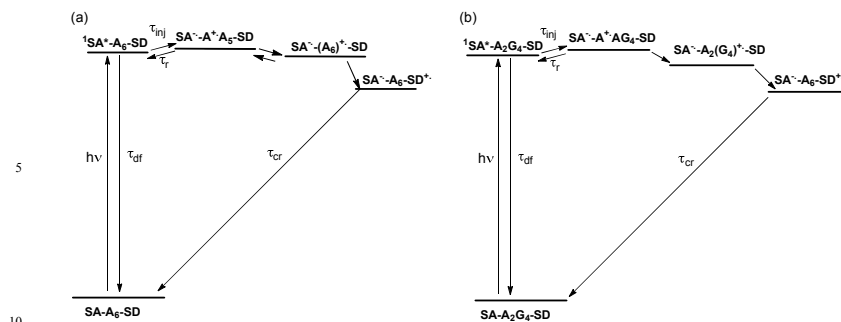
**Scheme 2.** Energetics and dynamics for hole injection and charge recombination in capped hairpins possessing a SA linker and SD capping group and an $A_6$ (a) or $A_2G_4$ (b) purine base sequence.

**Table 2:** Quantum yields for charge separation and kinetics for charge separation and charge recombination for NDI–SD capped hairpins from this study in aqueous buffer (0.1 M NaCl and 10 mM sodium phosphate, pH 7.2). Values in *()* are relative population of $NDI^{\cdot-}$ based on the 490 nm peak in the femtosecond transient absorption spectra. Values in () are relative population of $SD^{\cdot+}$ based on the 530 nm peak in the nanosecond transient absorption spectra.

| Capped Hairpin | $\Phi_{cs}^{a}$ | $\tau_{inj}$, ps[b] | $\tau_{r1}$, ps[b] | $\tau_{cs}$, ns[c] | $\tau_{r2}$, μs[d] |
|---|---|---|---|---|---|
| SA–SD–1[e] | 0.09 | | | 1 | 170 |
| SA–SD–2[e] | 0.32 | | | 9 | |
| NDI–SD–1 | 0.13 | <0.2 | 4.2 *(87)* | 0.025 | 17 *(13)* |
| NDI–SD–2 | 0.19 | <0.2 | 3.3 (70), 49 *(11)* | 0.20 | 64 *(19)* |
| NDI–SD–3 | 0.10 | ca. 1.0 | 6.6 *(90)* | 0.053 (48), 870 (52) | 1000 *(10)* |
| NDI–SD–4 | 0.30 | ca. 1.0 | 3.3 *(44)*, 35 *(26)* | 0.28 (70), 430 (30) | 200 *(30)* |

[a] Quantum yields for charge separation (Φcs) were estimated by comparing the integrated band intensities of the transient absorption spectra at long delay times with those for SA–Sd or NDI–SD capped hairpin with only one intervening AT base pair ($\Phi_{cs}$ =1.0). [b] Hole injection and prompt charge recombination times from femtosecond transient absorption measurements. [c] Sub-nanosecond charge separation times from femtosecond transient absorption measurements. Longer charge separation and charge recombination times from nanosecond measurements (see Experimental Section). [e] Data from refs. 26, 45.

mechanism.[26] The value of $\tau_{cr}$ for $SA^{\cdot-}A_2G_4SD^{+\cdot}$ has not been determined but is assumed to be similar to that for $SA^{\cdot-}A_6SD^{+\cdot}$.
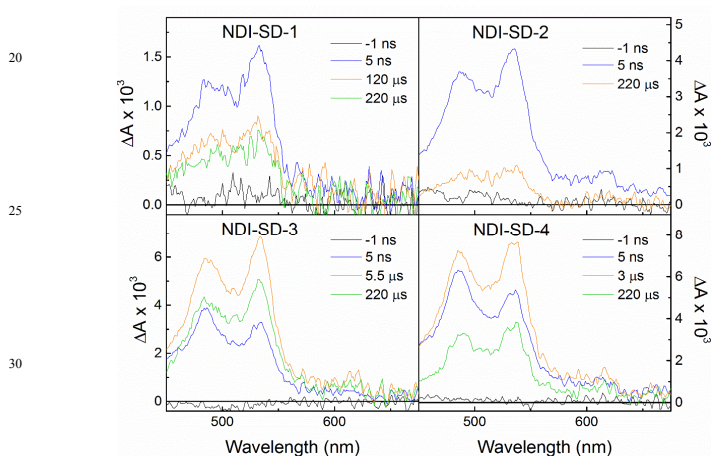
The transient absorption spectra of the capped hairpins **SA-SD-3** and **SA-SD-4** in which a X-X base pair has been inserted between the SA chromophore and adjacent A-T base pair (Chart 1c) are shown in Figure S3 (ESI). These spectra display no evidence for the formation of long-lived ($\tau > 6$ ns) charge separated states. The failure to observe hole transport via either an $A_6$ or $A_2G_4$ diblock purine sequence in the presence of an X-X base pair is consistent with the absence of hole injection in hairpin **SA-3**. Thus we conclude that the driving force for hole injection from $^1SA^*$ to A is not sufficient for hole injection when a X-X base pair is inserted between SA and the A-T base pair in either hairpin **SA-3** or the capped hairpins **SA-SD-3** or **SA-SD-4**. The absence of charge separation in **PDI-3** discouraged attempts to investigate the effects of a X-X base pair on charge separation in hairpins having a PDI hole donor and SD hole acceptor.

**2. Naphthalenediimide-linked capped hairpins**

Efficient quenching of $^1NDI^*$ fluorescence by the proximal A-T base pairs in hairpin **NDI-3** (Table 1) suggested that NDI could be employed as the hairpin linker for the
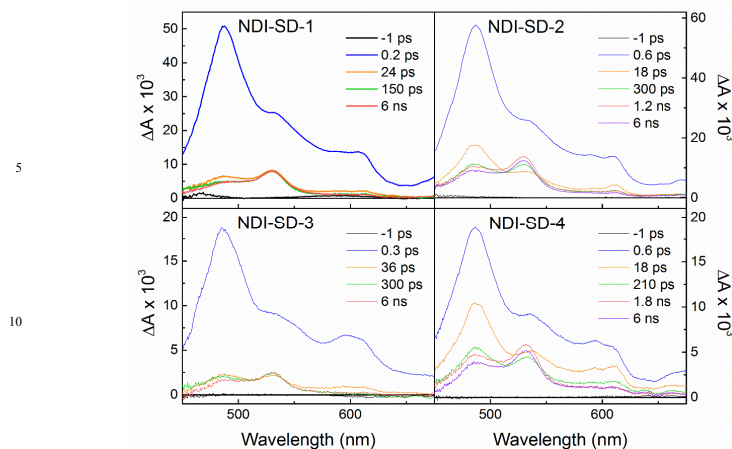
**Fig. 6** Femtosecond transient absorption spectra for NDI-linked capped hairpins **NDI–SD–1–4** in phosphate buffer (10 mM phosphate, 0.1 M NaCl, pH 7.2). Selected spectra at −1 ps, a time point right after the instrument response, points at $\tau*6$, and a final time point at the extent of the time window.



**Fig. 7** Nanosecond ttransient absorption spectra for NDI-linked capped hairpins **NDI–SD–1–4** in phosphate buffer (10 mM phosphate, 0.1 M NaCl, pH 7.2). Selected spectra at −1 ns, a time point at 5 ns, roughly after the femtosecond time window, points at $\tau*6$, and a final time point at the extent of the time window.

study of the dynamics of charge separation and recombination in capped hairpins **NDI-SD-3** and **NDI-SD-4** (Chart 1c). Femtosecond and nanosecond time-resolved transient absorption spectra for **NDI-SD-1-4** are shown in Figures 6 and 7, respectively. The spectra at short delay times following laser excitation (< 1 ps) are similar to those for **NDI-1** (Figure 5), indicative of fast hole injection both in the absence and in the presence of the X-X base pair ($\tau_{inj}$, Table 2). At longer delay times the maximum near 535 nm assigned to $SD^{+\cdot}$ becomes prominent and does not decay appreciably on the 7 ns time scale of the femtosecond measurements. The time constants for charge separation ($\tau_{cs}$) obtained from the rise time of the 535 nm transient are reported in Table 2. The long-lived decays of both the $NDI^{-\cdot}$ and $SD^{+\cdot}$
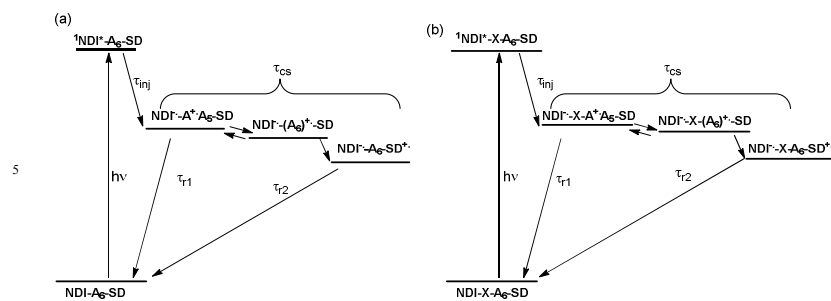
**Scheme 3.** Energetics and dynamics for hole injection and charge recombination in capped hairpins possessing a NDI linker and SD capping group and an $A_6$ purine base sequence (a) without and (b) with an X-X artificial base pair.

bands are attributed to charge recombination of the charge separated states ($k_{r2}$, Table 2). The short lived decays of $NDI^-$ which occur prior to the formation of $SD^{+\cdot}$ ($k_{r1}$, Table 2) are attributed to charge recombination of the $NDI^-/A^{+\cdot}$ or $NDI^-X-A^{+\cdot}$ radical ion pairs.

The values of $\tau_{inj}$ and $\tau_{r1}$ for **NDI-SD-1-4** are similar to the values of $\tau_{inj}$ and the major short-lived component of $\tau_{cr}$ for **NDI-1**. Thus the presence of the X-X base pairs in **NDI-SD-3** or **NDI-SD-4** does not have a large effect on the dynamics of highly exergonic hole injection or charge return processes in these hairpins ($\tau_{ing}$ and $\tau_{r1}$, Scheme 3b). This conclusion is consistent with the small increases in fluorescence intensity for **NDI-SD-3** and **NDI-SD-4** vs. **NDI-SD-1** and **NDI-SD-2** (Figure 2c). In the case of **NDI-SD-3** charge separation is biexponential, the short lived component having a value of $\tau_{cs}$ similar to that for **NDI-SD-1** and the second component having a substantially longer rise time. Both of the values of $\tau_{cs}$ for **NDI-SD-4** are substantially longer than the values for **NDI-SD-2**. The charge recombination times $\tau_{r2}$ for **NDI-SD-3** and **NDI-SD-4** are also substantially longer than the values for **NDI-SD-1** and **NDI-SD-2**. A plausible explanation for slow charge separation and charge recombination (but not hole injection and charge return) is that the X-X base pair disrupts base stacking in the $A_6$ and $A_2G_4$ poly(purine) hole transport sequences. Structural analysis of a duplex containing an artificial base pair consisting of a 4-isopropylcyclohexl- and a 4-methyl-cyclohexyl-D-threoninol located between A-T and G-C base pairs shows that the cyclohexane rings are endo-helical and do not "severely disturb" base pairing of the natural nucleobases.[12] However, the effect of the X-X base pair on hairpin geometry has not been established. Alternatively, some of the $^1NDI^*$ may undergo intersystem crossing followed by triplet hole injection, resulting in spin-forbidding charge recombination.[46]

## 4. Concluding Remarks

The effect of an artificial X-X base pair on the fluorescence quantum yield and dynamics of photoinduced charge separation and charge recombination in DNA hairpins is dependent upon both the choice of hairpin linker chromophore and the adjacent purine base. Only in the case of a PDI hairpin linker are large increases in quantum yield observed for both guanine and adenine bases in the presence of an X-X base pair. For the SA linker a modest increase is observed with guanine but not adenine and for the NDI linker modest increases are observed with both adenine and

guanine. Only in the case of NDI are rapid charge separation and the formation of long-lived charge separated states observed in the presence of the X-X base pair. This suggests that the X-X base pair may find utility in systems for the efficient generation of long-lived charge separated states in DNA if appropriate design principles are followed.

## References

[a] *Address, Department of Chemistry, Northwestern University, Evanston, Illinois 60208-3113 USA. Tel: 1-847-491-3441: E-mail: fdl@northwestern.edu*

† Electronic Supplementary Information (ESI) available: MALDI-TOF mass spectra, melting temperatures, and CD spectra. Transient absorption spectra of NDI diol.. See DOI: 10.1039/b000000x/

1. M. R. Wasielewski, *Chem. Rev.*, 1992, **92**, 435.
2. V. Balzani, *Electron Transfer in Chemistry*, Wiley-VCH, Weinheim, Germany, 2001.
3. B. Albinsson and J. Mårtensson, *J. Photochem. Photobiol. C Rev.*, 2008, **9**, 138.
4. O. S. Wenger, *Acc. Chem. Res.*, 2011, **44**, 25.
5. F. D. Lewis and Y. Wu, *J. Photochem. Photobiol. C: Rev.*, 2001, **2**, 1.
6. K. Kawai and T. Majima, *Acc. Chem. Res.*, 2013, **46**, 2616.
7. F. D. Lewis, *Israel J. Chem.*, 2013, **53**, 350.
8. J. C. Genereux and J. K. Barton, *Chem. Rev.*, 2010, **110**, 1642.
9. F. D. Lewis, X. Liu, S. E. Miller, R. T. Hayes and M. R. Wasielewski, *J. Am. Chem. Soc.*, 2002, **124**, 11280.
10. K. Kawai, Y. Osakada, M. Fujitsuka and T. Majima, *Chem. Eur. J.*, 2008, **14**, 3721.
11. H. Kashida, K. Sekiguchi and H. Asanuma, *Chem. Eur. J.*, 2010, **16**, 11554.
12. H. Kashida, K. Sekiguchi, N. Higashiyama, T. Kato and H. Asanuma, *Org. Biomol. Chem.*, 2011, **9**, 8313.
13. H. Kashida, N. Higashiyama, T. Kato and H. Asanuma, *Bioorg. Med. Chem.*, 2013, **21**, 6191.
14. F. D. Lewis, T. Wu, X. Liu, R. L. Letsinger, S. R. Greenfield, S. E. Miller and M. R. Wasielewski, *J. Am. Chem. Soc.*, 2000, **122**, 2889.
15. F. D. Lewis, Y. S. Wu, L. G. Zhang, X. B. Zuo, R. T. Hayes and M. R. Wasielewski, *J. Am. Chem. Soc.*, 2004, **126**, 8206.
16. R. L. Letsinger and T. Wu, *J. Am. Chem. Soc.*, 1995, **117**, 7323.
17. S. Bevers, T. P. O'Dea and L. W. McLaughlin, *J. Am. Chem. Soc.*, 1998, **120**, 11004.
18. M. Rahe, C. Rinn and T. Carell, *Chem. Commun.*, 2003, 2120.
19. W. H. Melhuish, *J. Phys. Chem.*, 1961, **65**, 229.
20. K. E. V. Brown, B. S.; Co, D. T.; Wasielewski, M. R. , *J.Phys. Chem. Lett.*, 2012, **3**, 2362.
21. S. M. D. R. M. Young, J. C. Barnes, M. Juricek, J. F. Stoddart, D. T. Co, M. R. Wasielewski, *J. Phys. Chem. A*, 2013, **117**, 12438
22. A. K. Mishra, R. M. Young, M. R. Wasielewski and F. D. Lewis, *J. Am. Chem. Soc.*, 2014, **136**, 15792.
23. W. C. Johnson, in *Circular Dichroism, Principles and Applications*, eds. N. Berova, K. Nakanishi and R. W. Woody, Wiley-VCH, New York, 2000, pp. 703.
24. M. Ardhammar, T. Kurucsev and B. Nordén, in *Circular Dichroism, Principles and Applications*, eds. N. Berova, K. Nakanishi and R. W. Woody, Wiley-VCH, New York, 2000, pp. 741.
25. M. Hariharan, Y. Zheng, H. Long, T. A. Zeidan, G. C. Schatz, J. Vura-Weis, M. R. Wasielewski, X. B. Zuo, D. M. Tiede and F. D. Lewis, *J. Am. Chem. Soc*, 2009, **131**, 5920.
26. F. D. Lewis, H. Zhu, P. Daublain, T. Fiebig, M. Raytchev, Q. Wang and V. Shafirovich, *J. Am. Chem. Soc.*, 2006, **128**, 791.
27. F. D. Lewis, H. Zhu, P. Daublain, K. Sigmund, T. Fiebig, M. Raytchev, Q. Wang and V. Shafirovich, *Photochem. Photobiol. Sci.*, 2008, **7**, 534.
28. A. Weller, *Zeit. Phys. Chem. Neue. Folg.*, 1982, **133**, 93.

29.  F. D. Lewis, L. Zhang, R. F. Kelley, D. McCamant and M. R. Wasielewski, *Tetrahedron*, 2007, **63**, 3457.

30.  S. Farid, J. P. Dinnocenzo, P. B. Merkel, R. H. Young and D. Shukla, *J. Am. Chem. Soc.*, 2011, **133**, 4791.

31.  C. A. M. Seidel, A. Schulz and M. H. M. Sauer, *J. Phys. Chem.*, 1996, **100**, 5541.

32.  J. Jortner, M. Bixon, T. Langenbacher and M. E. Michel-Beyerle, *Proc. Natl. Acad. Sci. U.S.A.*, 1998, **95**, 12759.

33.  E. M. Conwell and D. M. Basko, *J. Am. Chem. Soc.*, 2001, **123**, 11441.

34.  T. A. Zeidan, R. Carmieli, R. F. Kelley, T. M. Wilson, F. D. Lewis and M. R. Wasielewski, *J. Am. Chem. Soc.*, 2008, **130**, 13945.

35.  M. B. Zimmt and D. H. Waldeck, *J. Phys. Chem. A*, 2003, **107**, 3580.

36.  N. Prokopuk, K.-a. Son and C. Waltz, *J. Phys. Chem. C*, 2007, **111**, 6533.

37.  F. C. Grozema, S. Tonzani, Y. A. Berlin, G. C. Schatz, L. D. A. Siebbeles and M. A. Ratner, *J. Am. Chem. Soc.*, 2008, **130**, 5157.

38.  R. Carmieli, T. A. Zeidan, R. F. Kelley, Q. Mi, F. D. Lewis and M. R. Wasielewski, *J. Phys. Chem. A*, 2009, **113**, 4691.

39.  J. M. Giaimo, J. V. Lockard, L. E. Sinks, A. M. Vega, T. M. Wilson and M. R. Wasielewski, *J. Phys. Chem. A.*, 2008, **112**, 2322.

40.  T. A. Zeidan, R. Carmieli, R. F. Kelley, T. M. Wilson, F. D. Lewis and M. R. Wasielewski, *J. Am. Chem. Soc.*, 2008, **130**, 13945.

41.  F. D. Lewis, R. S. Kalgutkar, Y. Wu, X. Liu, J. Liu, R. T. Hayes and M. R. Wasielewski, *J. Am. Chem. Soc.*, 2000, **122**, 12346.

42.  T. Takada, K. Kawai, X. Cai, A. Sugimoto, M. Fujitsuka and T. Majima, *J. Am. Chem. Soc.*, 2004, **126**, 1125.

43.  P. Ganesan, J. Baggerman, H. Zhang, E. J. R. Sudhölter and H. Zuilhof, *J. Phys. Chem. A*, 2007, **111**, 6151.

44.  M. Supur, M. E. El-Khouly, J. H. Seok, K.-Y. Kay and S. Fukuzumi, *J. Phys. Chem. A*, 2011, **115**, 14430.

45.  J. Vura-Weis, M. R. Wasielewski, A. K. Thazhathveetil and F. D. Lewis, *J. Am. Chem. Soc.*, 2009, **131**, 9722.

46.  R. Carmieli, A. L. Smeigh, S. M. Mickley Conron, A. K. Thazhathveetil, M. Fuki, Y. Kobori, F. D. Lewis and M. R. Wasielewski, *J. Am. Chem. Soc.*, 2012, **134**, 11251.

**Faraday Discussions Accepted Manuscript**